Journal of Applied Polymer Science

Synthesis of Cationic Magnetite Nanoparticles for Intracellular Protein Delivery

Zheng Wang,[1] Jianjun Zhang,[2] Ruiduan Li,[2] Jianfeng Chen[2]

[1]General Hospital of PLA, Beijing 100853, China

[2]State Key Laboratory of Organic-Inorganic Composites, Beijing University of Chemical Technology, Beijing 100029, China

Correspondence to: J. Zhang (E-mail: zhangjj@mail.buct.edu.cn)

ABSTRACT: Intracellular protein delivery shows great promise in the treatment of various diseases. However, therapeutic applications of this method are limited by its low delivery efficiency and poor targeting ability. As one of most important drug delivery cargoes, Fe_3O_4 nanoparticles (nFe_3O_4) have attracted much attention for both therapeutic and diagnostic applications, especially for targeting drug delivery. To use nFe_3O_4 for protein delivery, a simple but effective modification of nFe_3O_4 is critical to attach proteins on its surface. In this work, by designing and synthesizing cationic poly(2-(dimethylamino)ethyl methacrylate) (PDMA)-grafted nFe_3O_4 via *in situ* atom transfer radical polymerization (ATRP), we demonstrate a simple solution to improve interactions between nFe_3O_4 and proteins. With the grafted PDMA on the surface, nFe_3O_4 exhibits not only significant enhancement in dispersibility and stability in aqueous phase, but also an excellent capability to attach negative-charged proteins. Moreover, with the assistance of external magnetic field, PDMA-grafted nFe_3O_4 can be used as a targetable vector to deliver proteins into specific cells. This work provides a novel platform based on cationic magnetite nanoparticles that can deliver therapeutic proteins into specific sites for the treatment of various diseases. © 2013 Wiley Periodicals, Inc. J. Appl. Polym. Sci. **2014**, *131*, 40260.

KEYWORDS: drug delivery systems; proteins; radical polymerization; nanoparticles; nanowires and nanocrystals; magnetism and magnetic properties

Received 1 September 2013; accepted 5 November 2013

DOI: 10.1002/app.40260

INTRODUCTION

Intracellular protein delivery shows great promise in the treatment of various diseases.[1–4] To date, several promising vectors, such as cell-penetrating peptides (CPPs),[5–9] liposomes or cationic polymers,[10–16] have been used to deliver functional proteins into cells to rectify cellular functions. The protein/CPPs conjugates are able to translocate into cells with significant delivery efficiency, but they are susceptible to denaturation and degradation during endocytosis. Liposomes can assist proteins delivery with good protection during endocytosis but low efficiency. Cationic polymers have shown high efficiency as delivery vectors by assembling proteins through noncovalent interactions or covalent conjugation. However, cationic polymer vectors cannot achieve the purpose of the site-specific delivery of proteins. Recently, Fe_3O_4 nanoparticles (nFe_3O_4) have attracted much attention for their therapeutic and diagnostic applications due to their potential targeting property.[17–28] However, their wide applications are hampered by the weak interaction with bio-molecules. Therefore, a simple but effective modification on nFe_3O_4 surface to improve interactions between nanoparticles and bio-molecules is very important.[29]

To date, the surface modification of nFe_3O_4 has been explored by either direct conjugation or *in situ* growth of polymer chains on the surface.[30–32] Atom transfer radical polymerization (ATRP), an *in situ* polymerization technique synthesizing polymers with narrow molecular mass distribution, desired composition and molecular architecture,[33,34] is particularly useful for the synthesis of hybrid polymer-nFe_3O_4, such as (P(PEGMA))-grafted nFe_3O_4,[35] PNIPAAm-coated nFe_3O_4 and nFe_3O_4@-PHEMA-g-PCL.[36,37] Nonetheless, using of such approach to modify cationic polymer on the surface of nFe_3O_4 for attaching negative-charged proteins by electrostatic effect and further delivering proteins into targetable cells by the control of external magnetic field has not been achieved.

Herein, we present a novel intracellular protein delivery system based on cationic poly(2-(dimethylamino)ethyl methacrylate) (PDMA)-grafted nFe_3O_4. This is the first report about using nFe_3O_4 grafted positively charged PDMA polymer for protein delivery. Positively charged PDMA was first grafted on nFe_3O_4 surface by *in situ* atom transfer radical polymerization (*in situ* ATRP) to obtain cationic nFe_3O_4 [Figure 1(a,b)]. After the graft of PDMA, nFe_3O_4 acquire excellent dispersibility in aqueous

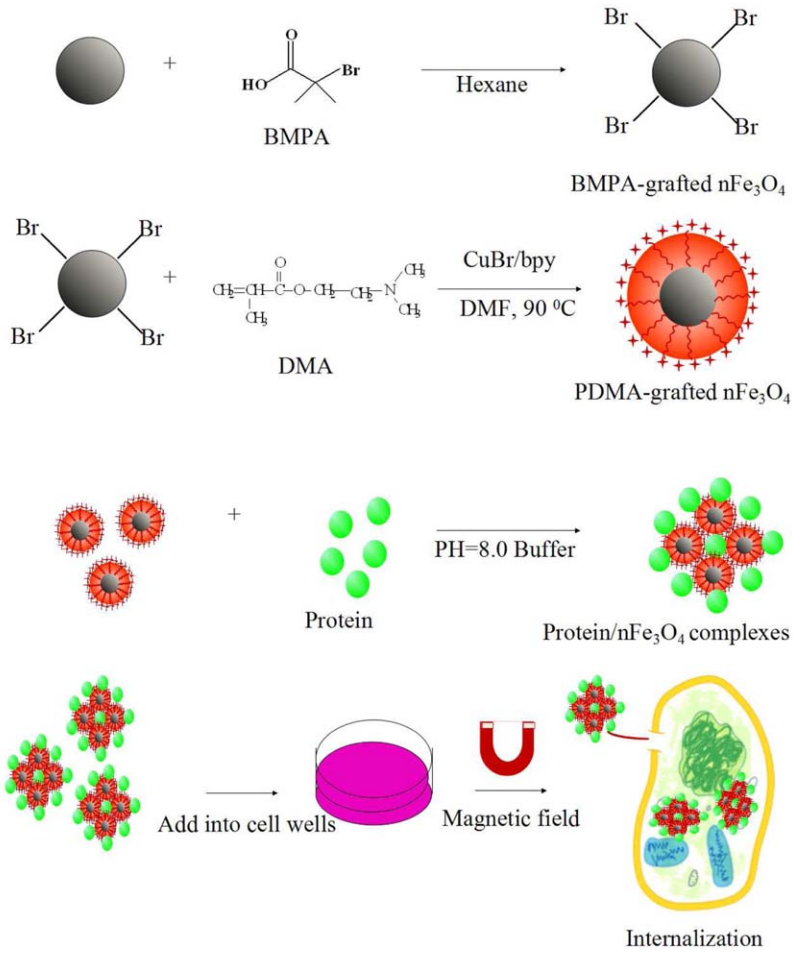

Figure 1. Schematic illustration showing the synthesis and cellular uptake of protein/nFe_3O_4 complexes. (a) Ligand exchange of nFe_3O_4; (b) Synthesis of PDMA-grafted nFe_3O_4 by *in situ* ATRP; (c) Positively charged nFe_3O_4 and negatively charged BSA assembled into amorphous complexes by electrostatic effect; (d) Cellular uptake of protein/nFe_3O_4 complexes by external magnetic field. [Color figure can be viewed in the online issue, which is available at wileyonlinelibrary.com.]

phase and are ability to attach negative-charged proteins by electrostatic interaction [Figure 1(c)]. Rhodamine-B-labeled BSA and EGFP were used as model proteins to form protein/nFe_3O_4 complexes and with the assistance of external magnetic fields protein/nFe_3O_4 complexes were internalized by cells [Figure 1(d)]. It was hypothesized that the delivery of these complexes to cells would be divided into two steps. First, the complexes were attached on cells by magnetic field under the cell wells, and then the complexes were internalized into cells by endocytosis way. By achieving directed delivery, the cationic PDMA-grafted nFe_3O_4 show their potentiality for site-specific delivery of proteins.

EXPERIMENTAL

Materials

Benzyl ether, *N*,*N*-dimethylformamide (DMF, anhydrous, 99.8%), 1,2-hexadecanediol, oleic acid, oleylamine, iron (III) acetylacetonate, 2-bromo-2-methylpropionic acid (BMPA), 2,2′-bipyridyl (Bpy), copper (I) bromide, rhodamine B isothiocyanate, bovine serum albumin (BSA) protein and lipase from thermomyces lanuginosus were purchased from Aldrich–Chemical and used as received. Enhanced green fluorescent protein (EGFP) was expressed according to previous reports.[38] 2-(dimethylamino)ethyl methacrylate (DMA) was passed through a basic alumina column, and then distilled prior to polymerization.

Synthesis of nFe_3O_4

nFe_3O_4 were prepared according to a previously reported method [30]: iron (III) acetylacetonate (1.05 g, 3 mmol), 1,2-hexadecanediol (3.87 g, 15 mmol), oleic acid (2.42 g, 9 mmol), oleylamine (2.42 g, 9 mmol), and benzyl ether (30 mL) were mixed and magnetically stirred under a flow of nitrogen. The mixture was heated at 200°C for 2 h, and then heated with reflux (300°C) under nitrogen for another 1 h. When the black mixture was cooled down to room temperature, amount of ethanol was added to the mixture, and then black precipitate was separated via centrifugation (5000 rpm). The black product was redissolved in 20 mL of hexane, then precipitated with ethanol again, and collected by centrifugation (4000 rpm, 15 min). The process was repeated three times to purify the product. Finally, nFe_3O_4 were dried under reduced pressure and stored at 4°C.

Ligand Exchange of nFe_3O_4

About 60 mg of nFe_3O_4 were dispersed in 10 mL of 2*M* BMPA in hexane and stirred for a week at room temperature under the protection of argon. The resulting black precipitate was separated using a centrifuge at 10,000 rpm for 15 min and washed three times with hexane to remove the excess initiator. The BMPA grafted nFe_3O_4 were then dried under reduced pressure and stored at 4°C.

In Situ Atom Transfer Radical Polymerization on the Surface of nFe_3O_4

The BMPA grafted nFe_3O_4 (10 mg), 2 mL of DMA and 20 mL of DMF were added into a 100 mL Schlenk flask with a magnetic stir bar. The reagent mixture was purged under argon for 30 min and degassed by five freeze-pump-thaw cycles. CuBr (10 mg) and bpy (20 mg) were dissolved in 1 mL of DMF, which was purged under argon, and then injected into a flask via syringe. The flask was heated to 90°C in oil bath for 12 h. The PDMA-grafted nFe_3O_4 were separated by using a centrifuge at 10,000 rpm for 15 min and washed three times with DMF to remove the excess monomer and impurity. The PDMA-grafted nFe_3O_4 were then dried under reduced pressure and stored at 4°C.

Attaching of Proteins to PDMA-Grafted nFe_3O_4

Amount of PDMA-grafted nFe_3O_4 (0.2, 0.4, and 0.8 mg) were added to 2 mL of boric acid buffer (pH 8.0, 20 m*M*) containing 0.1 mg mL^{-1} protein and stirred for 4 h. The protein/nFe_3O_4 complexes were separated via magnetic field and washed three times with boric buffer to remove unattached proteins. Finally, the complexes were freeze-dried and stored at 4°C.

Cell Internalization *In Vitro*

Cellular internalization studies were assessed via fluorescence microscopy. HeLa cells were cultured in Dulbecco's modified Eagle's medium (DMEM) supplemented with 10% fetal bovine serum (FBS) and 1% penicillin. Cells (35,000 cells $well^{-1}$, 24-well plate) were seeded the day before adding rhodamine-B-labeled BSA/nFe_3O_4 and EGFP/nFe_3O_4 complexes. The protein/nFe_3O_4 complexes were added into cell wells with and without external magnetic field under the plate at final concentration of 0.4 mg mL^{-1}. After incubation at 37°C for 1 h, the cells were washed three times with PBS and assessed with a fluorescent microscope and fluorescence-activated cell sorting (FACS).

In Vitro Cytotoxicity Assay

In vitro cytotoxicity of protein/nFe_3O_4 complexes was evaluated by the 3-(4,5-dimethylthiazol-2-yl)-2,5-diphenyltetrazolium bromide (MTT) assay. HeLa cells (7000 cells per well, 96-well plate) were seeded the day before adding PDMA-grafted nFe_3O_4 and protein/nFe_3O_4 complexes. Various concentrations of PDMA-grafted nFe_3O_4 and protein/nFe_3O_4 complexes were added into cell wells with an external magnetic field under the plate. After incubation at 37°C for 1 h, the cells were washed three times with PBS to remove free samples and incubated for another 24 h. Nearly 20 μL of MTT solution (5 mg mL^{-1} in PBS) was added into each well and incubated for 4 h. The absorbance reading was measured at 560 nm by microplate reader. The relative cell viability compared to the control cell culture in the absence of complexes. All the testing was performed in triplicate.

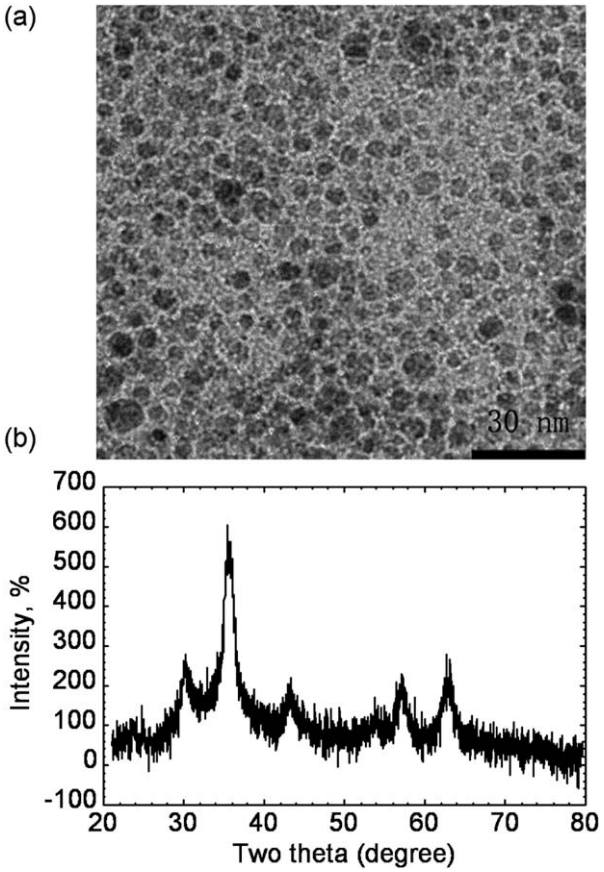

Figure 2. (a) TEM image and (b) X-ray diffraction pattern of oleic acid-stabilized nFe_3O_4 prepared from thermal decomposition process.

Characterization

The morphologies of the nanoparticles were subsequently determined by TEM on a Philips EM120 TEM at 100,000×. Fourier transform infrared (FT-IR) spectra were obtained with a Bruker FT-IR spectrometer using KBr disks. Zeta potential and average particle size distribution were measured with a MALVERN NANO-ZS Zeta-Sizer. Crystalline structure was examined using an X-ray diffractometer (XRD-6000 diffractometer, Shimadzu, Japan). Fluorescence images of cells were obtained with a fluorescence microscope (Zeiss, Observer.Z1). Thermogravimetric analysis (TGA) was performed on a PerkinElmer thermal analysis.

RESULTS AND DISCUSSION

nFe_3O_4 prepared by the thermal decomposition process possessed uniform particle size, eximious magnetism and high chemical stability. Figure 2(a) shows transmission electron microscopy (TEM) image of nFe_3O_4 prepared by the high temperature decomposition of iron acetylacetonate with oleic acids as ligands. The resulted nFe_3O_4 are quite uniform with an average size of ~6 nm. Furthermore, X-ray diffraction (XRD) result clearly shows characteristic diffraction patterns of nFe_3O_4 with high degree of crystallinity [Figure 2(b)].

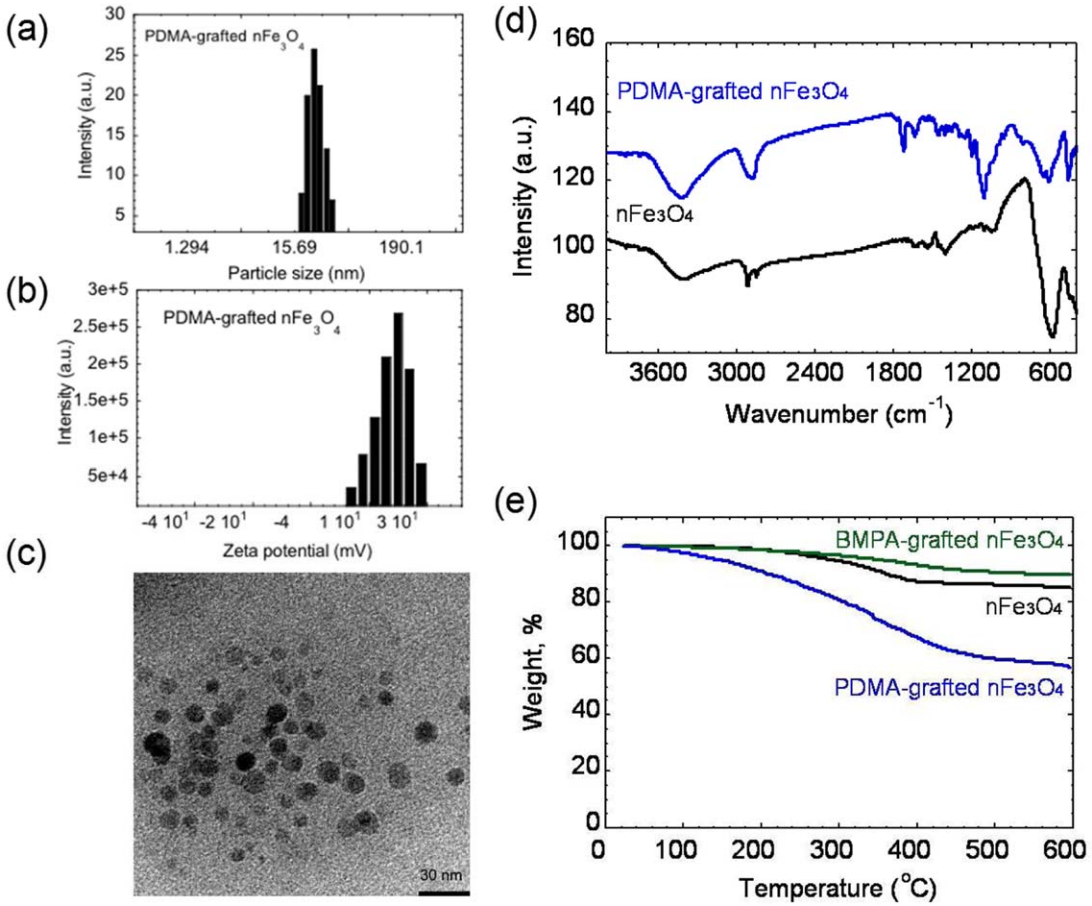

Figure 3. Characterization of PDMA-grafted nFe_3O_4. (a) Particle size, (b) zeta potential and (c) TEM image of PDMA-grafted nFe3O4. (d) FT-IR spectrums of oleic acid-stabilized and PDMA-grafted nFe_3O_4, and (e) TGA curves of oleic acid-stabilized, BMPA grafted and PDMA-grafted nFe_3O_4. [Color figure can be viewed in the online issue, which is available at wileyonlinelibrary.com.]

The oleic acid-stabilized nFe_3O_4 dispersed well in nonpolar solvents, such as hexane and toluene. However, after stirred in a hexane solution containing the initiator BMPA for 72 h, the collected nFe_3O_4 were not able to redisperse in hexane, but still showed good solubility in polar solvents, such as THF, DMF, or ethanol. This observation indicated that these modified nFe_3O_4 had different surface chemistry from the initial oleic acid-stabilized ones, indicating the successful ligand exchange with BMPA. The BMPA on nFe_3O_4 were then used as an initiator to induce *in situ* ATRP with DMA monomer to form cationic PDMA-grafted nFe_3O_4. The formation of cationic PDMA-grafted nFe_3O_4 was confirmed by TEM, DLS, Zeta potential, FT-IR and TGA. Compared with the oleic acid-stabilized nFe_3O_4, the PDMA-grafted nFe_3O_4 exhibit increased average size of ~24.2 nm [Figure 3(a)]. Because polymer shell is not discernible due to the lack of contrast with the background, only the metal oxide core of the PDMA-grafted nFe_3O_4 can be observed in TEM image [Figure 3(c)].[35] Moreover, as show in Figure 3(b), after grafting PDMA, nFe_3O_4 exhibit a positive surface potential of +16.5. The characteristic FT-IR absorption of PDMA at 1729 cm^{-1} (the carbonyl group) and 1148 cm^{-1} (C—N stretching) [Figure 3(d)] is only observed on PDMA-grafted nFe_3O_4, confirming the formation of PDMA chains during the polymerization. To further investigate the surface modification of nFe_3O_4 with PDMA, the thermal gravimetric analysis (TGA) results are summarized in Figure 3(e). The gravimetric losses of 14.3, 15.2, and 41.1% at 600°C were observed for oleic acid-stabilized, BMPA-grafted and

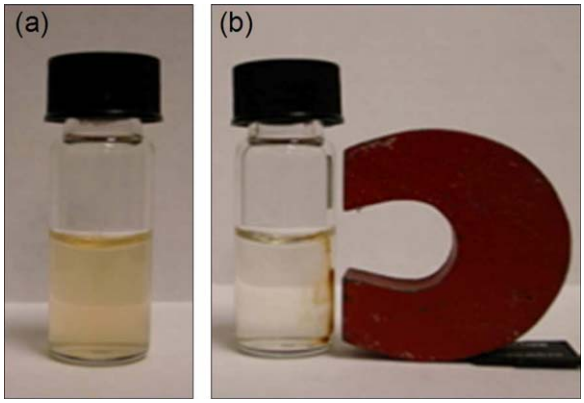

Figure 4. Photographs of (a) PDMA-grafted nFe_3O_4 dispersing in aqueous-phase and (b) PDMA-grafted nFe_3O_4 in aqueous-phase with external magnetic field. [Color figure can be viewed in the online issue, which is available at wileyonlinelibrary.com.]

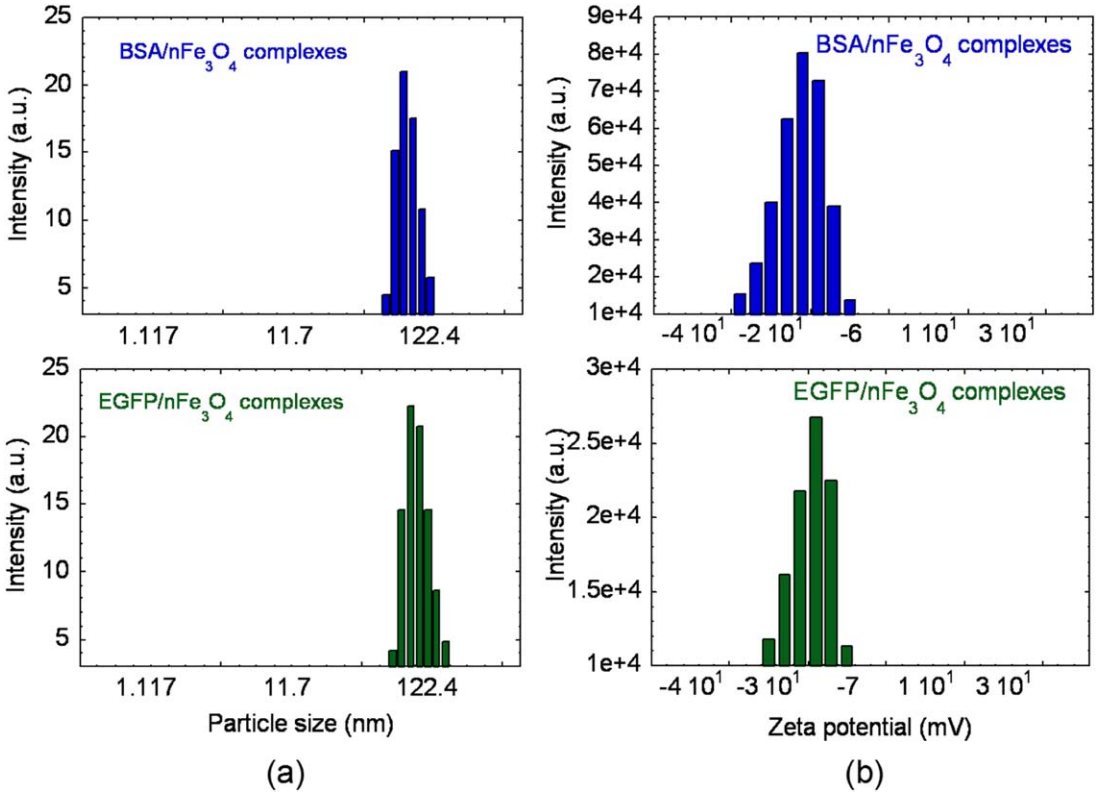

Figure 5. Particle size (a) and zeta potentials (b) of BSA/nFe_3O_4 complexes and EGFP/nFe_3O_4 complexes. (c) TEM image of BSA/nFe_3O_4 complexes. [Color figure can be viewed in the online issue, which is available at wileyonlinelibrary.com.]

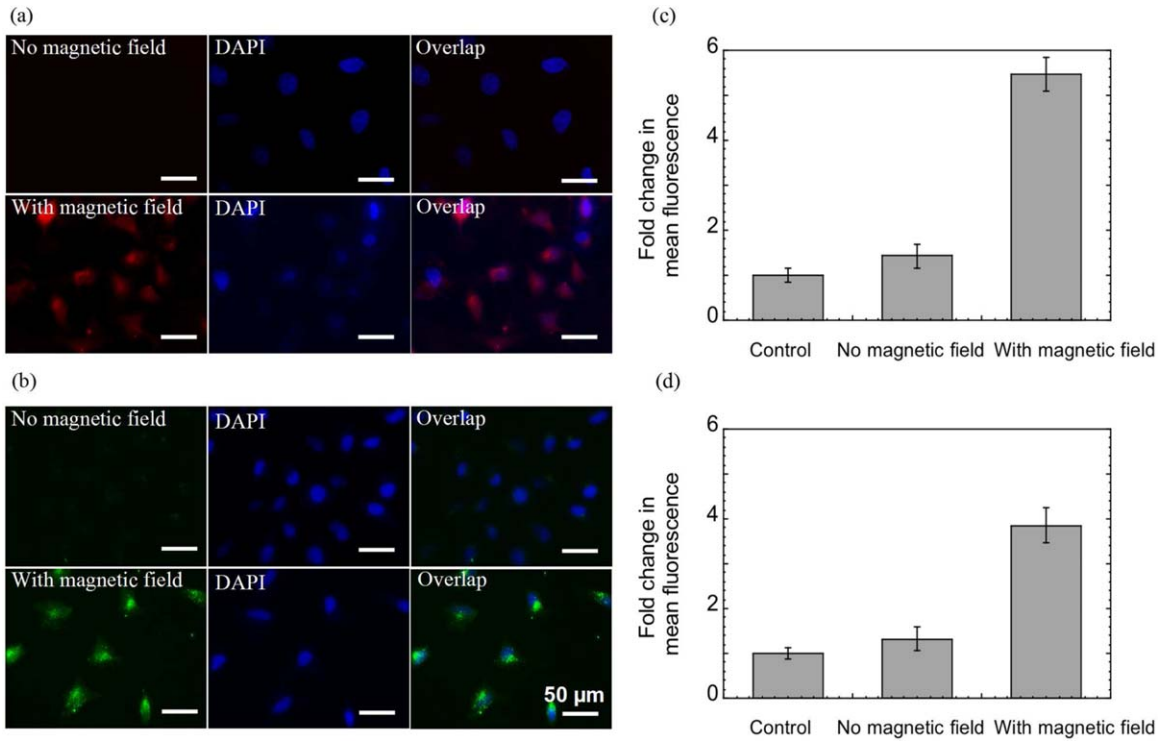

Figure 6. Fluorescence images of cellular uptake of Rhodamine-B-labeled BSA/nFe_3O_4 complexes (a) and EGFP/nFe_3O_4 complexes (b) at the concentration of 0.4 mg mL^{-1} without and with external magnetic field. [Color figure can be viewed in the online issue, which is available at wileyonlinelibrary.com.]

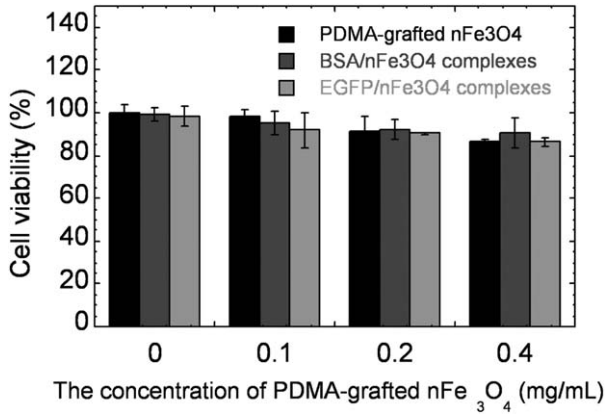

Figure 7. Cell viability of HeLa cells after treatment with PDMA-grafted nFe_3O_4, BSA/nFe_3O_4 complexes and EGFP/nFe_3O_4 complexes at various concentrations of 0, 0.1, 0.2, 0.4 mg mL^{-1}.

PDMA-grafted nFe_3O_4, respectively. According to TGA results, the gravimetric losses of both oleic acid-stabilized and BMPA-grafted nFe_3O_4 were much less than that of PDMA-grafted nFe_3O_4, which could be ascribed to more organic components on the surface of PDMA-grafted nFe_3O_4.

Grafting PDMA on nFe_3O_4 surface significantly enhanced the particles dispersibility. Figure 4(a) shows PDMA-grafted nFe_3O_4 dispersing in aqueous solution. Despite the graft of PDMA polymer, magnetic nFe_3O_4 were still sensitive to magnetic field. Figure 4(b) demonstrates that well-dispersed PDMA-grafted nFe_3O_4 can response to an applied external magnetic field, indicating their potential applications as vectors for site-specific drug delivery.

Owing to the graft of positively charged PDMA, nFe_3O_4 were able to attach negatively charged proteins via electrostatic interactions. BSA and EGFP, which presented negative surface charge at physiological pH region of 7–8, were chosen as model proteins. Figure 5(a,b) show the particle size and surface charge of these two kinds of protein/nFe_3O_4 complexes. Average diameters of 78.5 and 90.7 nm and zeta potentials of −13.5 and −11.2 mV are observed for BSA/nFe_3O_4 and EGFP/nFe_3O_4 complexes, respectively. The results demonstrated that the PDMA-grafted nFe_3O_4 successfully assembles with negative-charged proteins, resulting in increased particle size and negative surface charge. Figure 5(c) shows TEM image of BSA/nFe_3O_4 complexes, indicating that positively charged nFe_3O_4 and negatively charged BSA assembled into amorphous complexes with a diameter in the range of 50–100 nm.

Moreover, the use of external magnetic field enabled directed intracellular delivery of the complexes. Rhodamine-B-labeled BSA and EGFP were chosen as models for cellular uptake. Figure 6(a,b) show the fluorescence images of HeLa cells preincubated with Rhodamine-B-labeled BSA/nFe_3O_4 and EGFP/nFe_3O_4 complexes without or with external magnetic field. The cells incubated with magnetic field show significantly high fluorescence intensity from proteins is observed in the cells incubated under magnetic field for both complexes. The FACS results of HeLa cells preincubated with Rhodamine-B-labeled BSA/nFe_3O_4 and EGFP/nFe_3O_4 complexes with and without external magnetic field are shown in Figure 6(c,d). Compared with the complexes without external magnetic field the complexes with an external magnetic field have fold increase in fluorescence intensity for both of Rhodamine-B-labeled BSA/nFe_3O_4 and EGFP/nFe_3O_4 complexes. The results of fluorescence images and FACS demonstrated that the cellular uptake of the complexes depends on the assistance of external magnetic fields and without the existence of magnetic fields; however, the intracellular delivery efficiency of the complexes are significantly reduced. It was hypothesized that the delivery of these complexes to cells would be divided into two steps. First, the complexes were attached on cells by magnetic field under the cell wells, and then the complexes were internalized into cells by endocytosis way.

The cytotoxicity of PDMA-grafted nFe_3O_4, BSA/nFe_3O_4, and EGFP/nFe_3O_4 complexes was assessed using the MTT assay. Figure 7 compares the viability of HeLa cells after exposure to various concentrations of PDMA-grafted nFe_3O_4, BSA/nFe_3O_4, and EGFP/nFe_3O_4 complexes. There are >80% cells remained alive even after treatment with a maximum sample concentration of 0.4 mg mL^{-1}, suggesting neglectable cytotoxicity of all samples.

CONCLUSION

In summary, cationic magnetite Fe_3O_4 nanoparticles (nFe_3O_4) were synthesized via grafting positively charged polymer on their surface. First, the macrointiator (BMPA) on the surface of nFe_3O_4 was introduced through ligand exchange. The following *in situ* ATRP yielded PDMA-grafted nFe_3O_4. These modified nFe_3O_4 possess good dispersibility and stability in aqueous phase. Moreover, the motion of the nanoparticles can be controlled by external magnetic fields. Owing to the grafting of cationic polymer, the nanoparticles enable to enrich negative-charged proteins (such as BSA and EGFP) by electrostatic interaction on their surface. Furthermore, under external magnetic fields, the protein/nFe_3O_4 complexes are efficiently internalized by HeLa cells with low cytotoxicity. This work provides a robust platform for delivering therapeutic proteins, such as HRP,[39] RNase,[16] and growth factor,[40] to the targeted organs or tissues by localized external magnetic fields. Moreover, we believe that such a synthesis strategy is not limited to nFe_3O_4; it can be adapted to widely functional nanoparticles for various therapeutic applications.

ACKNOWLEDGMENTS

The authors thank the Chinese University Scientific Fund (ZY-1202), National Natural Science Foundation of China (51303009), and National Basic Research Program of China (973 Program) (2012CB933900) for financial support.

REFERENCES

1. Birch, J. R.; Onakunle, Y. Therapeutic Proteins, Methods and Protocols; Humanna Press, **2005**; p 1.
2. Wadia, J. S.; Becker-Hapak, M.; Dowdy, S. F. Cell-Penetrating Peptides: Processes and Applications. **2002**; p 365.

3. Choi, J. H.; Jang, J. Y.; Joung, Y. K.; Kwon, M. H.; Park, K. D. *J Controlled Release* **2010**, *147*, 420.
4. Khalil, I. A.; Kogure, K.; Futaki, S.; Harashima, H. *Int. J. Pharm.* **2008**, *354*, 39.
5. Torchilin, V. P. *Pept. Sci.* **2008**, *90*, 604.
6. Sawant, R.; Torchilin, V. *Mol. BioSys.* **2010**, *6*, 628.
7. Chugh, A.; Eudes, F.; Shim, Y. S. *IUBMB Life.* **2010**, *62*, 183.
8. Sato, H.; Sugiyama, Y.; Tsuji, A.; Horikoshi, I. *Adv. Drug Deliv. Rev.* **1996**, *19*, 445.
9. Vyas, S. P.; Singh, A.; Sihorkar, V. *Crit. Rev. Ther. Drug. Carrier. Syst.* **2001**, *18*, 1.
10. Torchilin, V. P. *Nat. Rev. Drug. Discov.* **2005**, *4*, 145.
11. Bulmus, V.; Woodward, M.; Lin, L.; Murthy, N.; Stayton, P.; Hoffman, A. *J. Controlled Release* **2003**, *93*, 105.
12. Murata, H.; Futami, J.; Kitazoe, M.; Yonehara, T.; Nakanishi, H.; Kosaka, M.; Tada, H.; Sakaguchi, M.; Yagi, Y.; Seno, M.; Huh, N. H.; Yamada, H. *J. Biochem.* **2008**, *144*, 447.
13. Lee, A. L. Z.; Wang, Y.; Ye, W. H.; Yoon, H. S.; Chan, S. Y.; Yang, Y. Y. *Biomaterials* **2008**, *29*, 1224.
14. Futami, J.; Kitazoe, M.; Maeda, T.; Nukui, E.; Sakaguchi, M.; Kosaka, J.; Miyazaki, M.; Kosaka, M.; Tada, H.; Seno, M.; Sasaki, J.; Huh, N. H.; Namba, M.; Yamada, H. *J. Biosci. Bioeng.* **2005**, *99*, 95.
15. Didenko, V. V.; Ngo, H.; Baskin, D. S. *Anal. Biochem.* **2005**, *344*, 168.
16. Zhang, J.; Du, J.; Yan, M.; Dhaliwal, A.; Wen, J.; Liu, F.; Segura, T.; Lu, Y. *Nano Res.* **2011**, *4*, 425.
17. Lee, H.; Lee, E.; Kim, D. K.; Jang, N. K.; Jeong, Y. Y.; Jon, S. *J. Am. Chem. Soc.* **2006**, *128*, 7383.
18. Mornet, S.; Vasseur, S.; Grasset, F.; Veverka, P.; Goglio, G.; Demourgues, A. *Prog. Solid. State. Chem.* **2006**, *34*, 237.
19. Thorek, L. J. D.; Chen, A. K.; Czupryna, J.; Tsourkas, A. *Ann. Biomed. Eng.* **2006**, *34*, 23.
20. Ito, A.; Ino, K.; Kobayashi, T.; Honda, H. *Biomaterials* **2005**, *26*, 6185.
21. Sincai, M.; Ganga, D.; Ganga, M.; Argherie, D.; Bica, D. *J. Magn. Magn. Mater.* **2005**, *293*, 438.
22. Morishita, N.; Nakagami, H.; Morishita, R. *Biochem. Biophys. Res. Commun.* **2005**, *334*, 1121.
23. Neuberger, T.; Schopf, B.; Hofmann, H.; Hofmann, M.; Rechenberg, B. V. *J. Magn. Magn. Mater.* **2005**, *293*, 483.
24. Berry, C. C.; Curtis, A. S. G. *J. Phys. D. Appl. Phys.* **2003**, *36*, 198.
25. Shirly, B. D. M.; Riam, A. M.; Sara, R.; Haim, B.; Aharon, G. *Small* **2008**, *4*, 1453.
26. Lee, J.; Lee, Y.; Youn, J. K.; Na, H. B.; Yu, T.; Kim, H.; Lee, S. M.; Koo, Y. M.; Kwak, J. H.; Park, H. G.; Chang, H. N.; Hwang, M.; Park, J. G.; Kim, J.; Hyeon, T. *Small* **2008**, *4*, 143.
27. Dyal, A.; Loos, K.; Noto, M.; Chang, S. W.; Spagnoli, C.; Shafi, K. V. P. M.; Ulman, A.; Cowman, M.; Gross, R. A. *J. Am. Chem. Soc.* **2003**, *125*, 1684.
28. Guedes, M. H. A.; Sadeghiani, N.; Peixoto, D. L. G. *J. Magn. Magn. Mater.* **2005**, *293*, 283.
29. McBain, C. S.; Yiu, H. P. H.; Dobson, J. *Int. J. Nanomed.* **2008**, *3*, 169.
30. Kim, K. D.; Kim, S. S.; Choa, Y. H.; Kim, H. T. *J. Ind. Eng. Chem.* **2007**, *13*, 1137.
31. Vestal, C.; Zhang, Z. J. *J. Am. Chem. Soc.* **2002**, *124*, 14312.
32. Wang, Y.; Teng, X.; Wang, J. S.; Yang, H. *Nano. Lett.* **2003**, *3*, 789.
33. Matyjaszewski, K.; Xia, J. H. *Chem. Rev.* **2001**, *101*, 2921.
34. Tsarevsky, N. V.; Matyjaszewski, K. *Chem. Rev.* **2007**, *107*, 2270.
35. Fana, Q. L.; Neohb, K. G.; Kangb, E. T.; Shutera, B.; Wang, S. C. *Biomaterials* **2007**, *28*, 5426.
36. Frimpong, R. A.; Hilt, J. Z. *Nanotechnology* **2008**, *19*, 175101.
37. Yuan, W.; Yuan, J.; Zhou, L.; Wu, S.; Hong, X. *Polymer* **2010**, *51*, 2540.
38. Caron, N. J. *Mol. Ther.* **2001**, *3*, 310.
39. Yan, M.; Du, J.; Gu, Z.; Liang, M.; Hu, Y.; Zhang, W.; Priceman, S.; Wu, L.; Zhou, Z. H.; Liu, Z.; Segura, T.; Tang, Y.; Lu, Y. *Nat. Nanotech.* **2010**, *5*, 48.
40. Lee, K.; Silva, A. E.; Mooney, J. D. J. R. *Soc. Interface.* **2011**, *8*, 153.